2022 Moscow Workshop on Electronic and Networking Technologies (MWENT)

Analysis of Discrete Data Transmission and Noise Immunity in a Short-Range UHF Radio Channel

Vladimir Mikhaylovich Artyushenko
Information technology and management systems department
Technological University
Korolev city, Russian Federation
artuschenko@mail.ru

Vladimir Ivanovich Volovach
Informational and electronic service department
Volga Region State University of Service
Togliatty city, Russian Federation
volovach.vi@mail.ru

***Abstract*—Obtaining sufficiently high bandwidth and noise immunity of transmitted discrete data is achieved by using a super-high-frequency short-range radio channel. The features of duplex data exchange between various sensors of the system, as well as an algorithm for detecting their communication establishment are described. The probabilities of correct and false detection are found for this algorithm. It is shown that the speed of movement of the mobile module located on the vehicle, as well as the radio visibility range of the point sensor will determine the amount of transmitted data. The characteristic dependences for the radio visibility range are given. It is shown that noise immunity of the radio line can be described by the probability of error when transmitting a signal element. It is shown that signal fading caused by interference of direct and reflected from the underlying surface fields in the receiving aperture is critical for the noise immunity of the short-range radio channel. An expression for determining the modulus of the attenuation multiplier is obtained. The error probability is found for the case of a uniform distribution of the signal phase. The noise immunity of the radio line during fading of the received signal is determined for cases of a steady "shiny" point and of a large number of equivalent reflection points. The dependences of the error probability during signal transmission are obtained, taking into account both the value of the signal/noise ratio and the actual conditions of propagation of electromagnetic waves including reflections from the underlying surface.**

Keywords*—*microwave range, short-range radio channel, underlying surface, radio visibility range, error probability, bandwidth, signal fading, noise immunity

I. Introduction

When creating automated traffic control systems for vehicles (V), the task of reading or exchanging data between a moving vehicle and a stationary point located in a certain local spatial area is of vital importance. For example, performing such a task is necessary when building a system of automatic collection of primary data about the movement of goods on the railway network, when creating an automated control system for the movement of underground trains, buses, trams, etc. [1-4, etc.]. Although this problem is not difficult from a scientific point of view, however, very often operating conditions of such systems, for example, railway transport, turn out to be so complex that many simple solutions do not meet the requirements.

Experience has shown that in order to adjust the vehicle movement program and transmit various kinds of current data, it is most convenient to use the ultra-high frequency range (UHF), which has a number of advantages both in terms of noise immunity and technical implementation. The use of the microwave band makes it possible to organize a communication channel almost "closed" for the effects of external interference, thus to make it work at its full capacity.

As a rule, the distance between the transmitting and receiving microwave device does not exceed several meters, and the exchange of information is carried out during the stop, although, if necessary, it can be carried out during the movement of the vehicle [5-8, etc.]. The exchange of operational information between a vehicle and a stationary point can be both duplex and simplex, carried out using so-called point sensors (PS).

The aim of the work is to analyze the features of construction and operation of short-range microwave radio channel (SRMRC) using point sensors of duplex exchange of discrete information, including the algorithm of detection of communication of the named sensors and determination of interference immunity of radio link at deadlocks of received signal.

Let us consider and analyze the features of the construction and functioning of point sensors for data exchange.

II. A Point Sensor for Information Exchange

Since such sensors include two transmitters and receivers, and the distance between them is relatively small, such sensors can be regarded as the simplest radio channel with a small range.

The set of equipment [8] includes mobile and stationary half-sets, including M1 and M2 modulators, low frequency generators LFG, super high frequency signal generators SHFG and horn antennas HA on the transmitting side. On the receiving side there is a matching device MD, a limiting amplifier LA and a detector D.

The operation of the radio line is carried out as follows. A control discrete sequence is sent from data transmission equipment (DTE) on board the vehicle to the modulator M of the transmitter starting from a certain point in time. A modulated microwave signal is emitted by the HA antenna towards the installation site of the stationary half-set. Since the distance between the receiver and the transmitter is small, the receiver is built according to the direct gain scheme. The floor receiver detects the control sequence, which means entering into communication, after which the transmitter of the stationary set is switched on. Similarly, the connection of the receiver of the mobile set is carried out.

The difference in the polarization of channels of the duplex radio line makes it possible to eliminate mutual influences.

Synchronization of transmitted discrete sequences is carried out using clock and cycle synchronization systems, which are part of DTE.

Note that more complex types of modulation can also be used to ensure high noise immunity.

Identify applicable funding agency here. If none, delete this text box.

978-1-6654-9666-7/22/$31.00 ©2022 IEEE

An important characteristic of data exchange sensors is the radio visibility zone l_p, which is understood as an extent of the spatial area in which data can be exchanged between the floor and on-board sets. The radio visibility zone is determined by the direction of the antenna θ and the distance between the receiving and transmitting antennas R_0 (Fig. 1).

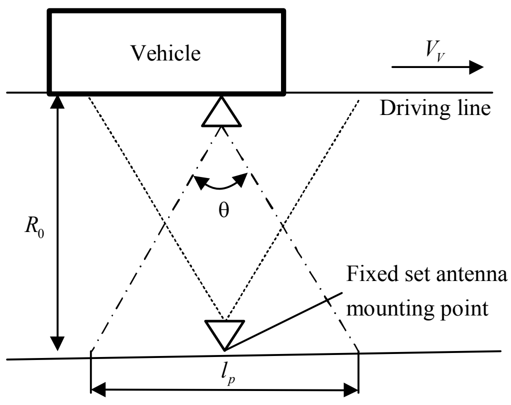

Fig. 1. Geometrical arrangement of the antennas of the data exchange sensors

If the vehicle is moving at a speed V_V along a line normal to the direction of radiation, then the radio visibility zone will be determined based on the expression

$$l_p = 2R_0 \mathrm{tg}(\theta/2).$$

Figure 2 shows the dependence of the radio visibility zone l_p in the horizontal plane for a pyramidal horn antenna with the following characteristics: the length of the horn R_E in the plane E: R_E = 5λ, where λ is the wavelength of the microwave signal; the size of the output section of the antenna aperture b_p = 0.08 m; the angle of the horn antenna aperture in the plane E: $2\varphi_{oE} = 5°$ with respect to R_0 [9].

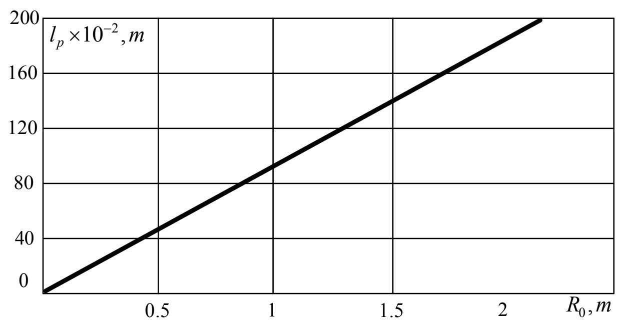

Fig. 2. Dependence of the radio visibility zone on the distance between the receiving and transmitting antennas

Knowing the value l_p and the speed V_V of the vehicle, it is easy to calculate the time of data exchange

$$t = l_p / V_V .$$

The dependences t on V_V and on R_0 are shown in Fig. 3.

So, for example, when l_p = 2 m and V_V = 27.7 m/s (100 km/h), the transmission time of information is equal to $t = 7.2 \cdot 10^{-2}$ sec. Using DTE with a transmission rate of 9600 Baud means transmitting 600 bytes of information in one direction. That is, in radio lines of this type, the amount of data transmission and transmission time are limited. They can be increased either by increasing the transmission speed, or by increasing the radio visibility zone.

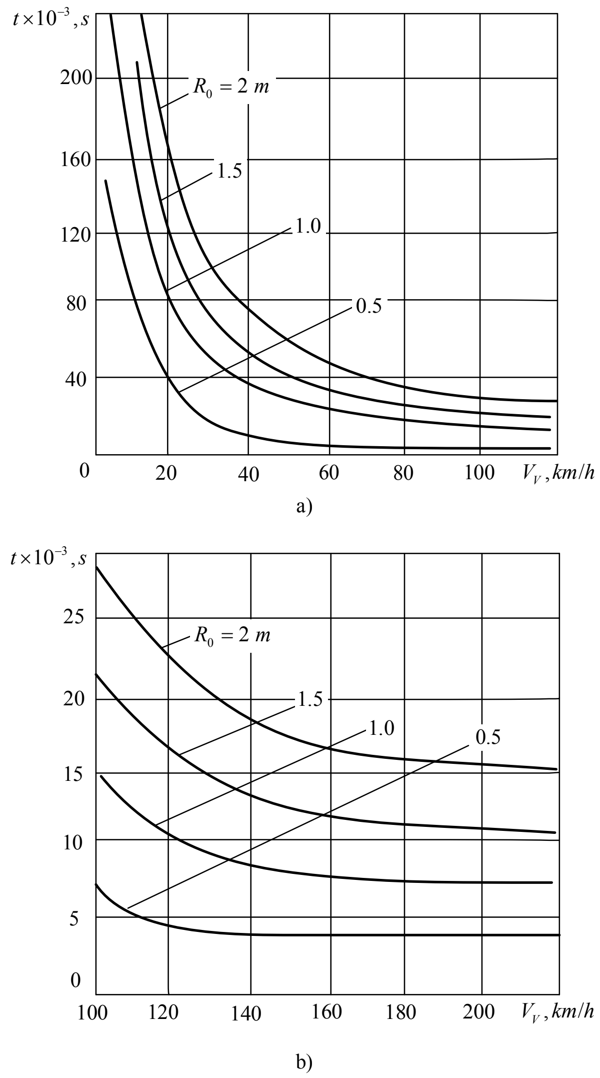

Fig. 3. Dependence of data exchange time on the vehicle speed, at different values of the distance between the receiving and transmitting antennas: a when the speed is V_V = 0…100 km/h, b at the speed V_V = 100…220 km/h

III. The Algorithm for Detecting Contact Establishment

The algorithm for detecting the fact of establishing the communication has the following form. Let the input of the threshold device (TD) receive a sequence of M samples u_i of voltage $u(t)$, which is a random process $y(t)$ at the output of the preprocessing unit of a mixture of the signal $s(t)$ and noise $n(t)$ $y(t) = s(t) + n(t)$, or noise $y(t) = n(t)$ only.

The counter turned on at the output of the TD sums up the number of samples N that have exceeded the threshold value U_{th} (in M samples), and the resolver (R) makes a decision on the presence or absence of the signal. For this purpose, the summation result N is compared with the threshold k_0. If $N \geq k_0$, then a decision is made about the presence of the signal. If $N < k_0$, then a decision is made about the absence of the signal.

We assume that all samples u_i are mutually independent, whereas the probability of a false alarm when making a decision based on one sample is assumed to be the same for all samples and is denoted as $(1 - p)$. Then the probability of a false alarm P_{FA} at the output of the described detector will be determined by the binary law of distribution of N in the absence of the signal in the samples u_i:

$$P_{FA} = \sum\nolimits_{l=k_0}^{M} C_M^l \left(1-p\right)^l p^{M-l},$$

where C_M^l is a number of combinations.

Suppose that the probability of exceeding the threshold level U_{th} in samples are equal to each other and are denoted as p, then the probability of correct detection P_{CD} will be determined based on the expression

$$P_{CD} = \sum\nolimits_{l=k_0}^{M} C_M^l \left(1-p\right)^{M-l} p^l.$$

It should be noted that the contribution to the value of each sample u_i due to the presence of the signal is generally different, since the signal can be present in an arbitrary number of samples M_s, not necessarily equal to M, that is $M_s \le M$. In addition, the signal strength due to fading may vary over time. In this case, the expressions for determining P_{CD} and P_{FA} are much more complex and can be determined only with the help of calculations performed with a personal computer.

IV. Noise immunity of the short-range radio line when the received signal fades

The noise immunity of the radio line will be characterized by the probability of an error when transmitting a signal element P_E. With incoherent reception, in the case of using amplitude modulation in the radio line, this probability can be found based on the expression [10]

$$P_E\left(q_s\right) = 0.5\exp\left\{-0,5 q_s^2 \left|A_r\right|\right\}. \tag{1}$$

Here $|A_r|$ is the modulus of the attenuation multiplier, which characterizes the real conditions of propagation of electromagnetic waves along a section of the radio line; $q_s^2 = 2P_sT/N_0^2$ plays the role of the signal/noise ratio (SNR), where P_s is the power of a signal element with duration T; N_0 is the spectral power density of noise.

It is known [4, 6] that at short range signal attenuation in the propagation area can be neglected.

Signal fading resulting from interference of direct $\dot{E}_d$ and reflected from the underlying surface $\dot{E}_r$ fields in the receiving aperture has a determining effect on the noise immunity of the radio line (Fig. 4).

Let us determine an attenuation multiplier A_r.

The total field intensity at the receiving point $\dot{E}_\Sigma$ will be determined as the sum of two components (2) where P_1, η_1, G_1 are, respectively, the radiation power, efficiency and gain of the antenna-feeder path of the transmitting antenna; $F_{tr}(\alpha)$, $F_{rec}(\beta)$ are, respectively, the directional characteristics of the transmitting and receiving antenna; α is the angle between the direction of maximum radiation and the direction to the center of the receiving aperture; β is the angle between the maximum radiation pattern of the receiving antenna and the pattern of the transmitting antenna; $\left|\Phi(x,y)\right|$, $\beta_\Phi(x, y)$ are respectively, the modulus and phase of the reflection coefficient, taking into account the decrease in amplitude and phase when reflecting electromagnetic waves from underlying surface; $C(x, y)$ is a current point with the coordinates (x, y) of the underlying surface $D(x, y)$ forming the reflected wave; α is the angle between the direction of maximum radiation and the direction to the center of the receiving aperture; β is an angle between the maximum of

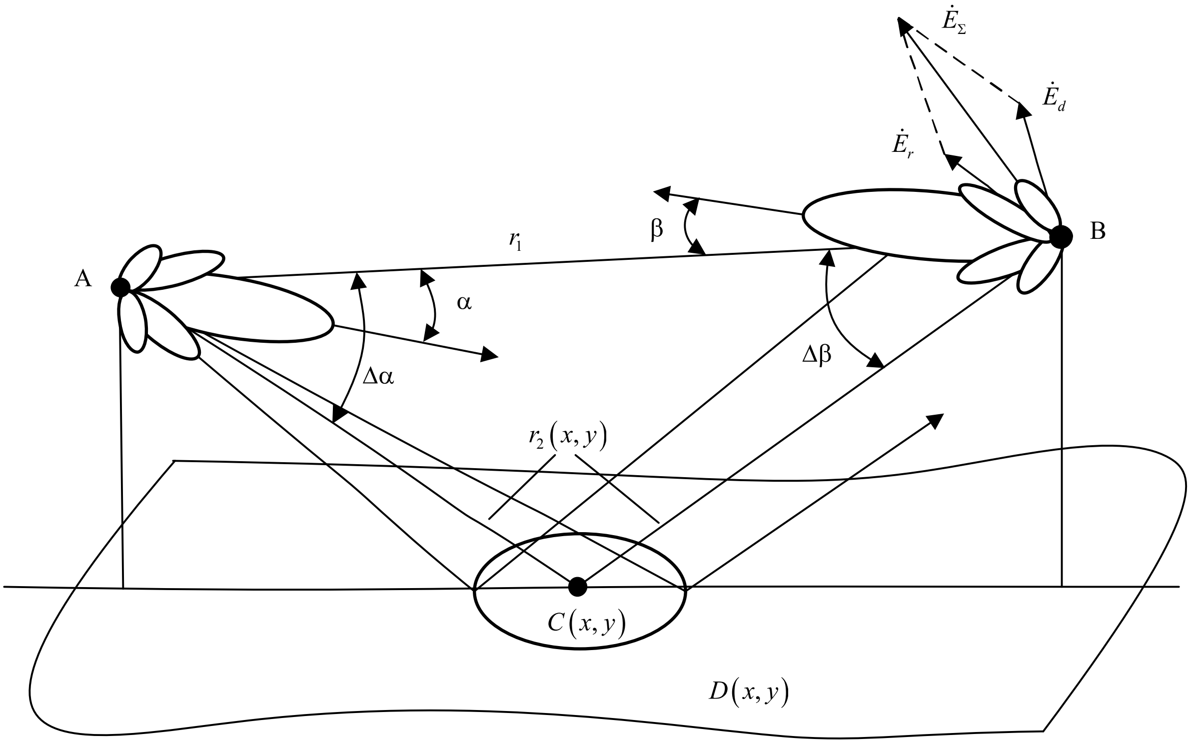

Fig. 4. Geometric explanation of the process of reflection from the underlying surface

$$\dot{E}_\Sigma = \dot{E}_d + \dot{E}_r = \frac{\sqrt{30P_1\eta_1G_1}}{r_1}F_{tr}(\alpha)\exp\{-ikr_1\}F_{rec}(\beta) + \\ + \int_{D(x,y)}|\Phi(x,y)|\frac{\sqrt{30P_1\eta_1G_1}}{r_2}F_{tr}[\alpha+\Delta\alpha(x,y)]F_d[\beta+\Delta\beta(x,y)]\exp\{-ikr_2 + i\beta_\Phi(x,y)\}ds(x,y). \quad (2)$$

the radiation pattern of the receiving antenna and the direction to the transmitting antenna; $r_1 = AB$, $r_2 = AC + CB$; $k = 2\pi/\lambda$. The angles $\Delta\alpha$ and $\Delta\beta$ are explained by Fig. 5

Assuming that $r_1^{-1} \approx r_2^{-1} \approx r^{-1}$, we transform expression (2) as

$$\dot{E}_\Sigma = \dot{E}_0\left[F_{tr}(\alpha)F_d(\beta) + J_1(\alpha,\Delta\alpha,\beta,\Delta\beta)\right], \quad (3)$$

where $\dot{E}_0 = \frac{1}{r}\sqrt{30P_1\eta_1G_1}\exp\{ikr_1\}$ is the intensity of the electromagnetic field during free space propagation of the signal;

$$J_1(\alpha,\Delta\alpha,\beta,\Delta\beta) = \\ = \int_{D(x,y)}F_{tr}[\alpha+\Delta\alpha(x,y)]F_d[\beta+\Delta\beta(x,y)]\times \\ \times|\Phi(x,y)|\exp\{i[k\Delta r(x,y)+\beta_\Phi(x,y)]\}ds(x,y);$$

$\Delta r(x, y)$ is the distance from the points A or B to the point $C(x, y)$ which forms the reflected wave and is located on the underlying surface $D(x, y)$.

According to [9], the expression in square brackets in formula (3) represents the attenuation multiplier characterizing the interference of direct and reflected waves, that is $\dot{E}_\Sigma = \dot{E}_0 A_r$.

For practical applications, the modulus of the attenuation multiplier is of greater interest

$$|A_r| = \{F^2(\alpha,\beta) + F^2(\alpha,\Delta\alpha,\beta,\Delta\beta)^2|\Phi^2(x,y)| + \\ +2F(\alpha,\beta)F(\alpha,\Delta\alpha,\beta,\Delta\beta)|\Phi(x,y)|\cos\varphi\}^{0.5}.$$

Here

$$F^2(\alpha,\beta) = F_{tr}(\alpha)F_d(\beta); \\ F(\alpha,\Delta\alpha,\beta,\Delta\beta) = F_{tr}(\alpha+\Delta\alpha)F_d(\beta+\Delta\beta); \\ \varphi = k\Delta r + \beta_\Phi.$$

By writing down:

$$a = F(\alpha,\beta);\quad b = F(\alpha,\Delta\alpha,\beta,\Delta\beta)|\Phi(x,y)|,$$

we transform expression (1) as

$$P_E = (q_s \mid a,b,\varphi) = 0.5\exp\{-0,5q_s^2(a^2+b^2+2ab)\cos\varphi\}.$$

We assume that the phase φ is evenly distributed:

$$\varphi \in W(\varphi) = \begin{cases} \frac{1}{2\pi}, & \text{if} \quad \varphi\in[-\pi,\pi]; \\ 0, & \text{if} \quad \varphi[-\pi,\pi], \end{cases}$$

where $W(\varphi)$ is the probability distribution function (PDF) of the phase.

Taking it into account, the probability of error will be determined based on the expression:

$$P_E = (q_s \mid a,b) = \int_{-\pi}^{\pi}P_E(q_s \mid a,b,\varphi)W(\varphi)d\varphi = \\ = I_0(a,b,q_s^2)\exp\{-0.5q_s^2(a^2+b^2)\}/4\pi, \quad (4)$$

where $I_0(.)$ is a zero-order Bessel function.

The first factor in expression (4) determines the random nature of the envelope of the signal reflected from the underlying surface. Since $D(x, y)$ can be regarded as an extended surface, the assumptions made about the PDF $W(b)$ can be the same as about extended targets considered in [11].

In practice, two reflection models are of the greatest interest: the one with a stable "shiny" point [12] and the one with a large number of equivalent reflection points.

In the first case

$$W(b) = \frac{b}{\sigma_b^2}\exp\left\{-\frac{b^2+a^2}{2\sigma_b^2}\right\}I_0(ba_b/\sigma_b^2), \quad (5)$$

where σ_B^2 is the variance of the coefficient b of the signal reflected from the surface $D(x, y)$; a_b is the value characterizing the mean of the coefficient b.

In the second case, when there is a large number of equivalent reflection points

$$W(b) = \frac{2m^m b^{2m-1}}{\Gamma(m)\sigma_b^{2m}}\exp\left\{-\frac{mb^2}{\sigma_b^2}\right\}, \quad (6)$$

where m is a distribution parameter; $\Gamma(.)$ is a gamma function.

Note that the PDF described by expression (6) is called a Nakagami distribution [13]. It is quite versatile. So, when m = 1, expression (6) becomes a Relay distribution [14], when $m > 1$, it becomes a generalized Relay distribution.

Substituting expression (5) into (4) and averaging over the parameter b, we find that the probability of error in this case will be defined as:

$$P_E = \int_0^\infty P_E(q_c \mid a,b)W(b)db = \\ = I_0\left[(a_b,a,q_c)/(\sigma_b^2q_c^2+1)\right]\sigma_b^2\times \\ \times\exp\left\{-Q/\left[2\pi(\sigma_b^2q_c^2+1)^2\right]\right\},$$

where

$$Q = \left[q_s^6a^2\sigma_b^4 + q_s^4\sigma_b^2(2a^2+2a_b^2) + \\ + q_s^2(2a^2\sigma_b^4 + a^2 + 2a_b^2) + a_b(2+\sigma_b^{-2})\right]\left[0.5(\sigma_b^2q_s^2+1)^2\right]^{-1}.$$

In the second case, when the PDF $W(b)$ is described by the Nakagami distribution (6), it can be shown that

$$P_E = m^m \exp\left\{-a^2 q_s^2/2\right\} \frac{{}_1F_1\left[m,1,-a^2 q_c^2/4\varkappa\right]}{4\pi\sigma_b^{2m}\varkappa^m}, \qquad (7)$$

where $\varkappa = \frac{1}{2}q_s^2 + \frac{m}{\sigma_b^2}$; ${}_1F_1[\alpha,\beta,\gamma]$ is a degenerate hypergeometric function.

If $m = 1$, that is, when the PDF $W(b)$ degenerate into a Rayleigh distribution, then

$${}_1F_1\left[m,1,-a^2 q_s^2/4\varkappa\right] = \exp\left\{-a^2 q_s^4/4\varkappa\right\}.$$

Expression (7) is simplified by follows

$$P_E = \frac{\exp\left\{-\frac{a^2 q_s^2}{2}\left[1+\frac{q_c^2}{2\varkappa}\right]\right\}}{4\pi\sigma_b^2\varkappa}.$$

In this case, the dependences of the probability of error during transmission of an elementary symbol on the value of the SNR will have the form shown in Fig. 5.

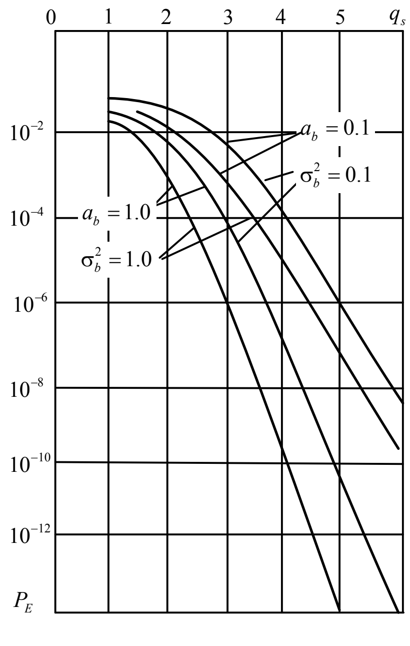

Fig. 5. The dependence of the probability of error on the value of the SNR at different values of σ_b^2 and a_b

The study showed that even when the SNR $q_c > 5$, the reliability of the data exchange sensor is very high. So, when $q_c = 5$; $a_b = 1.0$ and $\sigma_b^2 = 1.0$ the probability of error is $P_E \le 10^{-10}$.

V. Conclusion

Thus, the issues related to organizing the exchange of discrete information in an ultra-high-frequency short-range radio channel based on point sensors of data exchange are considered. The features of the construction and functioning of point sensors are analyzed. It is shown that radio lines based on them are short-range radio lines in which the volume of transmitted information and the transmission time are limited by the radio visibility zone of the point sensor and the speed of the vehicle.

The algorithm for detecting the fact that the data exchange point sensor enters into communication is considered, the noise immunity of the short-range radio line built on its basis with fading of the received signal is analyzed. We obtained the dependences of the probability of error during the transmission of a signal element on the signal/noise ratio at different values of the modulus of the attenuation multiplier which characterizes the real conditions of propagation of electromagnetic waves along the radio line section, as well as the reflection of electromagnetic waves from the underlying surface.

References

[1] Sergii Kliuiev, Ievgen Medvediev, Serhly Sorpka, and Vasyl Dubuk, “Development of the intelligent rail vehile control system”, 2020 IEEE 15th International Conference on Computer Sciences and Information Tecnologis (CSIT). Zbarazh, Ukraine, Sept 23-26, 2020. DOI: 10.1109/CSIT49958.2020.9321866

[2] I. Barankova, U. Mikhailova, and G. Lukianov, “Automated control system of a factory railway transport based on ZigBee”, 2016 2nd International Conference on Industrial Engineering, Applications and Manufacturing (ICIEAM). Chelyabibsk, Russia, 19-20 May, 2016. DOI: 10.1109/ICIEAM.2016.7910923

[3] I. F. Mikhalevich, “Problemic Issues of Deploying Cooperative Intelligent Transport Systems During of Digital Transformation”, 2021 Systems of Signals Generating and Processing in the Field of on Board Communications. Moscow, Russia, 16-18 March, 20. DOI: 10.1109/IEEECONF51389.2021.9415999

[4] Fei Yan, Tao Tang, and Hongwei Yan “Scenario based STPA analysis in Automated Urban Guided Transport system”, 2016 IEEE International Conference on Intelligent Rail Transportation (ICIRT). Birmingham, England, 23-25 Aug, 2016. DOI: 10.1109/ICIRT.2016.7588764

[5] G. L. Charvat Small and Short-Range Radar Systems. CRC Press, 2014.

[6] Jian Lan, and X. Rong Li, “Tracking of Extended Objects with High-Resolution Doppler Radar,” IEEE Trans. on Aerospace and Electronic Systems, 2016, Volume 52, Issue 6, pp. 2973–2989. https://doi.org/10.1109/TAES.2016.130346

[7] V. M. Artyushenko, and V. I. Volovach, “Calculating the Parameters of the Short-Range Microwave Information Channel Resistant to Signal Fading”, Proceedings of 2019 IEEE East-West Design & Test Symposium (EWDTS). Batumi, Georgia, Sept 13-16, 2019. – Kharkov: KNURE, 2019. P. 243-247. DOI: 10.1109/EWDTS.2019.8884399

[8] V. M. Artyushenko, and V. I. Volovach, “Analysis of Discrete Information Transmission in the Microwave Short-range Radio Line”, XIII International IEEE Scientific and Technical Conference “Dynamics of Systems, Mechanisms and Machines (Dynamics)”, Proceedings. Omsk: Omsk State Technical University, Omsk, Russia, Nov 5-7, 2019. DOI: 10.1109/Dynamics47113.2019.8944726

[9] David M. Pozar, Microwave Engineering, 4th ed., Wiley, 2012.

[10] M. Barkat, Signal Detection and Estimation. Norwood: Artech House, 2005.

[11] Habibur Rahman, Fundamental Principles of Radar, CRC Press, 2019.

[12] V. M. Artyushenko, and V. I. Volovach, “Estimation on motion Intensity of Extended Objects Using Generalized Weibull Distribution”, Optoelectronics, Instrumentation and Data Processing, May 2020 Vol. 56, Issue 3, pp. 261-268. DOI: 10.3103/S8756699020030024

[13] V. M. Artyushenko, and V. I. Volovach, “Nakagami Distribution Parameters Comparatively Estimated by the Moment and Maximum Likelihood Methods”, Optoelectronics, Instrumentation and Data Processing, May 2019, Vol. 55, Issue 3, pp. 237-242. DOI: 10.3103/S875669901903004X

[14] Mark Owen, Practical Signal Processing. Cambridge University Press, 2007.